3D Seismic Reflection Amplitude and Instantaneous Frequency Attributes in Mapping Thin Hydrocarbon Reservoir Lithofacies: Morrison NE Field and Morrison Field, Clark County, KS

ABDELMONEAM RAEF,[1] MATTHEW TOTTEN,[1] ANDREW VOHS,[1] and ARIA LINARES[1]

Abstract—Thin hydrocarbon reservoir facies pose resolution challenges and waveform-signature opportunities in seismic reservoir characterization and prospect identification. In this study, we present a case study, where instantaneous frequency variation in response to a thin hydrocarbon pay zone is analyzed and integrated with other independent information to explain drilling results and optimize future drilling decisions. In Morrison NE Field, some wells with poor economics have resulted from well-placement incognizant of reservoir heterogeneities. The study area in Clark County, Kanas, USA, has been covered by a surface 3D seismic reflection survey in 2010. The target horizon is the Viola limestone, which continues to produce from 7 of the 12 wells drilled within the survey area. Seismic attributes extraction and analyses were conducted with emphasis on instantaneous attributes and amplitude anomalies to better understand and predict reservoir heterogeneities and their control on hydrocarbon entrapment settings. We have identified a higher instantaneous frequency, lower amplitude seismic facies that is in good agreement with distinct lithofacies that exhibit better (higher porosity) reservoir properties, as inferred from well-log analysis and petrographic inspection of well cuttings. This study presents a pre-drilling, data-driven approach of identifying sub-resolution reservoir seismic facies in a carbonate formation. This workflow will assist in placing new development wells in other locations within the area. Our low amplitude high instantaneous frequency seismic reservoir facies have been corroborated by findings based on well logs, petrographic analysis data, and drilling results.

Key words: 3D seismic reflection, hydrocarbon reservoir, thin layers, instantaneous frequency, seismic amplitude.

1. Introduction

Analysis of P-wave 3D seismic reflection data attributes has been essential in many exploration and development projects around the world, particularly in terms of structural, petrophysical, and stratigraphic rock formation characterization. The main goal of an analysis of seismic attributes, such as root mean squared (RMS) amplitude, relative acoustic impedance, average energy and attenuation, curvature, coherency, time dip and dip azimuth, …etc., is to reveal litho- and/or petrophysical facies and relevance of structural and stratigraphic controls on reservoir quality aspects (e.g., Bunt 2015; Chen and Sidney 1997; Coléou et al. 2003; Raef et al. 2015, 2016; Wang et al. 2016). Instantaneous attributes such as instantaneous phase, instantaneous frequency, thin bed indicator, and normalized amplitude can aid in accurately tracking a horizon of interest throughout a seismic data volume, and also in determining zones of better reservoir properties. Thickening and thinning of strata can be recognized by animating through a series of frequencies along an interpreted horizon allowing an interpreter to identify where strata are thinning and thickening (Chopra and Marfurt 2008). Lateral continuity of events can be evaluated using instantaneous attributes like instantaneous phase, which is a useful attribute in indicating lateral continuity of rock layers and making a detailed visualization of bedding configurations, and it can make weakly coherent events more clear (Taner et al. 1979). A comprehensive classification of seismic attributes and the different modes of extraction and application are covered by Chen and Sidney (1997).

Seismic attributes based on the complex trace concept, Taner (2001), constitute a set of attributes that instantaneously and quantitatively describe the seismic waveform. Those attributes are derivable from a complex trace, $F(t)$, which is given by

$$F(t) = f(t) + jf_{\perp}(t) = A(t)e^{j\theta(t)},$$

where $f(t)$ is the real seismic trace, $f_{\perp}(t)$ is the

[1] Department of Geology, Kansas State University, 108 Thompson Hall, Manhattan, KS 66502, USA. E-mail: abraef@ksu.edu

imaginary or quadrature trace (Hilbert transform of $f(t)$), $A(t)$ is the instantaneous amplitude or reflection strength, and $\theta(t)$ is the instantaneous phase. Instantaneous frequency is defined as the rate of change of phase over time (derivative of instantaneous phase). Instantaneous frequency (f_{ins}) is calculated by the following equation:

$$f_{ins}(t) = \frac{d(\theta_{ins}(t))}{dt},$$

where $\theta_{ins}(t)$ is instantaneous phase and t is time (Sheriff and Geldart 1995).

In analyzing various seismic attributes, this study aims to determine if the main control on well productivity in the study area is related to preserved lithological facies during selective erosion due to original paleotopography as entrapment controls. The attributes analyzed reflect on an emphasis, which is placed on attributes that evaluate lithological heterogeneities, and attributes that give insight into the thinning and thickening of layers generating paleotopographic traps (Fig. 1).

A typical Viola limestone field was described by Richardson (2013) as the result of erosional paleotopographic relief, as schematically shown in Fig. 1, where the reservoir dolomite facies were preserved. This result in thinning and thickening of the net-pay, and in turn rendering it a good candidate for seismic attributes relevant to thinning-layer effects.

In December of 2010, Coral Coast Petroleum obtained a permit to begin drilling for hydrocarbons within the Morrison Northeast field and Morrison field in Clark County, Kansas. The development plan of this field was based on an interpretation of a P-wave 3D seismic reflection survey. Following the successful well completion of Stephens 1, 11 more wells were completed within the field. Seven of the wells drilled are still producing oil and/or gas from the Viola limestone. One well (initially dry and abandoned in the Viola) produces from the Morrow, three wells were dry holes, and a fifth marginally successful well targeting the Viola was converted into a salt water disposal (SWD) well. The survey also includes the location of the Harden 4 dry hole originally drilled by Berexco, Inc. in 2007; well locations of relevance are shown on maps in the subsequent sections.

2. Geologic Setting and Hydrocarbon Production Data

The Morrison and Morrison NE fields are located in east-central Clark County of Southwest Kansas within the Hugoton embayment which is a northern shelf-like extension of the Anadarko basin (Figs. 2, 3). The field is just west of the Central Kansas Uplift and the Pratt Anticline. Current hydrocarbon production is from the Ordovician aged Viola
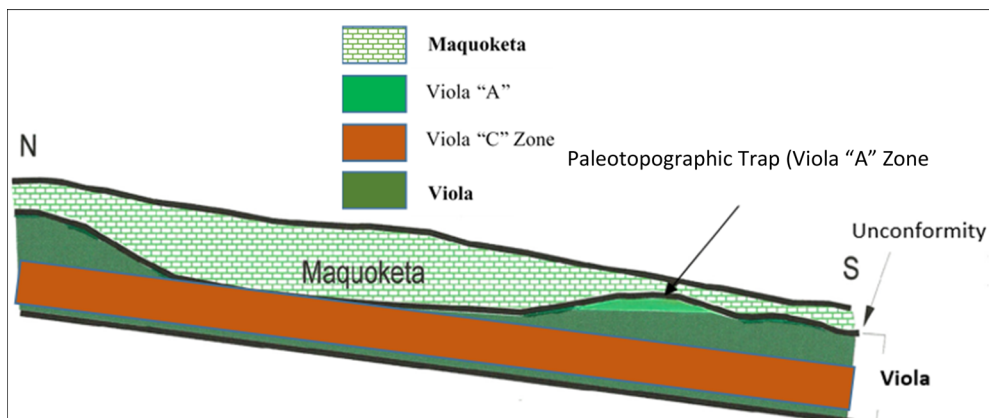

Figure 1
Idealized cross section showing paleotopographic traps within the Viola of the Herd Field, Comanche County, Kansas. The Herd Field is approximately 15 miles east of the study area. (Modified after Richardson 2013)
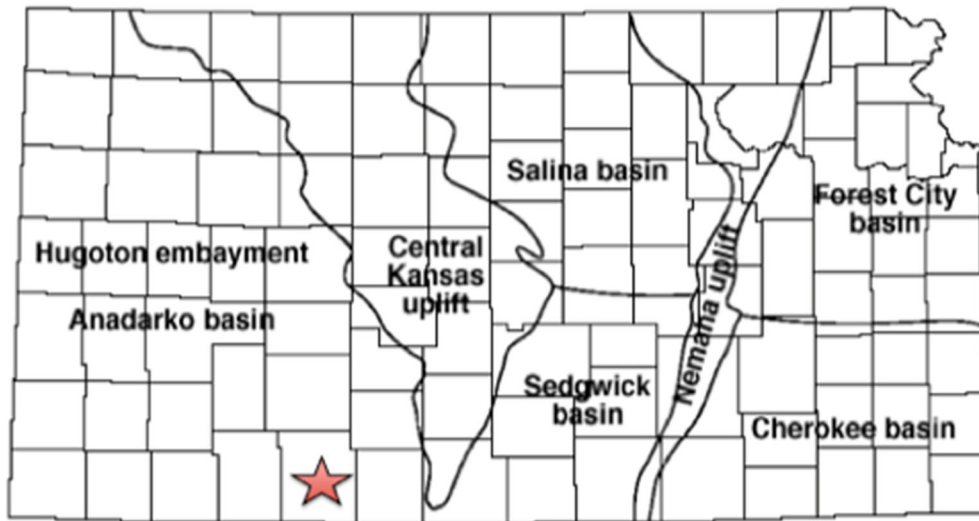
Figure 2
Location of Clark County, KS indicated by red star on this county map of Kansas, in relation with regional tectonic setting. (Adjusted from http://www.kshs.org, 2015)

Limestone, which is the formation of interest in this study.

The producing formation of the wells within the 3D seismic survey is the Middle Ordovician Viola limestone. Other formations of interest include the Upper Ordovician Maquoketa limestone, the Middle Ordovician Viola and Simpson groups, and the Lower Ordovician/Cambrian Arbuckle group. These four stratigraphic units are important to the study, because the Maquoketa and the Simpson bound the productive Viola formation above and below, respectively (Adkinson 1972). The Arbuckle group is important to this study, because its seismic signature is easy to track within the seismic data volume. This allows for accurate location and picking of other horizons of interest within the study area (Cole 1975).

Recognizing these strata on the well logs, as well as in the seismic section and petrographic thin sections is crucial in moving forward with this study to ensure horizons picked and attribute analysis is carried out at the correct time depth in the seismic section, along with the correct time to depth relationship when correlating the seismic facies to the stratigraphic lithofacies.

The Maquoketa limestone is a difficult to recognize but important unit with regard to Viola limestone production in the Morrison NE field. This limestone serves as the seal above the Viola limestone in the study area. The Maquoketa is a cream to light gray, dense limestone with no visible porosity and an average thickness of about 20–25 feet within the study area. The Maquoketa thins over paleotopographic highs of the Viola, and thickens in the lows. This dense non-porous rock makes an excellent seal for the petroleum system in the area (Richardson 2013).

The producing formation of the wells within the 3D seismic survey is the Ordovician Viola limestone. The Viola limestone was deposited in the middle Ordovician period in a warm tropical marine setting (Bornemann et al. 1982). The Viola varies between a fossiliferous limestone, and a medium to coarse crystalline vuggy dolomite, often containing scattered chert, with a total thickness of about 175–200 feet within the study area. It is informally divided into four distinct facies, delineated as the "A" through "D" zones. A stratigraphic column of the Viola within the study area is displayed in Fig. 4.

Vugs within the Viola "A" zone result in excellent porosity/permeability, which makes it an outstanding hydrocarbon reservoir rock (Goebel 1968). The Viola sits below an erosional unconformity representing about 20 Ma of subaerial exposure (St. Clair 1981), contributing to the formation of vugs that give the
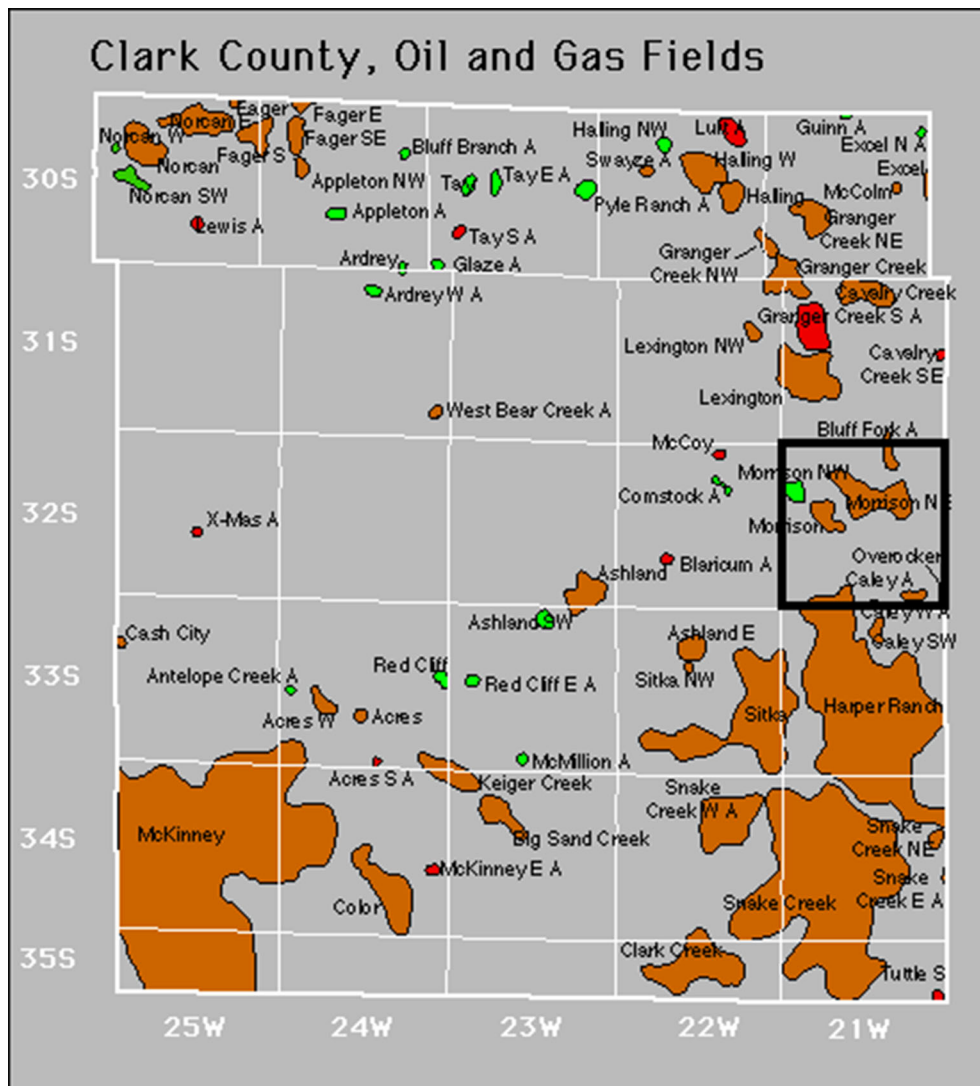
Figure 3
Clark County oil and gas fields, the Morrison, and Morrison NE fields are located in the east-central portion (marked with box) of the county (31S, 21W). (http://www.kgs.ku.edu/PRS/County/abc/clark.html: accessed, September 2016)

Viola "A" its good porosity and permeability. In some areas, the "A" zone and sometimes also the "B" zone are eroded away, resulting in a lack of reservoir conditions in non-productive limestone facies. Hence, the key to establishing production is determining, where the Viola "A" zone is preserved in a structurally favorable setting. An example of the resulting paleotopographic trap within the Viola as the result of this erosional unconformity in the analogous Herd Field is shown in Fig. 1 (Richardson 2013). The goal of this

research is to determine whether the productive Viola "A" zone may be recognized using seismic attributes.

Production within the Morrison NE field began in the 1950s with oil and gas being produced primarily from the Mississippian Limestone. In 2011, Coral Coast petroleum began producing oil and gas from the deeper Viola Limestone. The wells with a significant thickness of "A" zone (Stephens 1, 2, 4 and Harden 1) average over 70,000 barrels of cumulative oil production. Wells with a reduced thickness of this
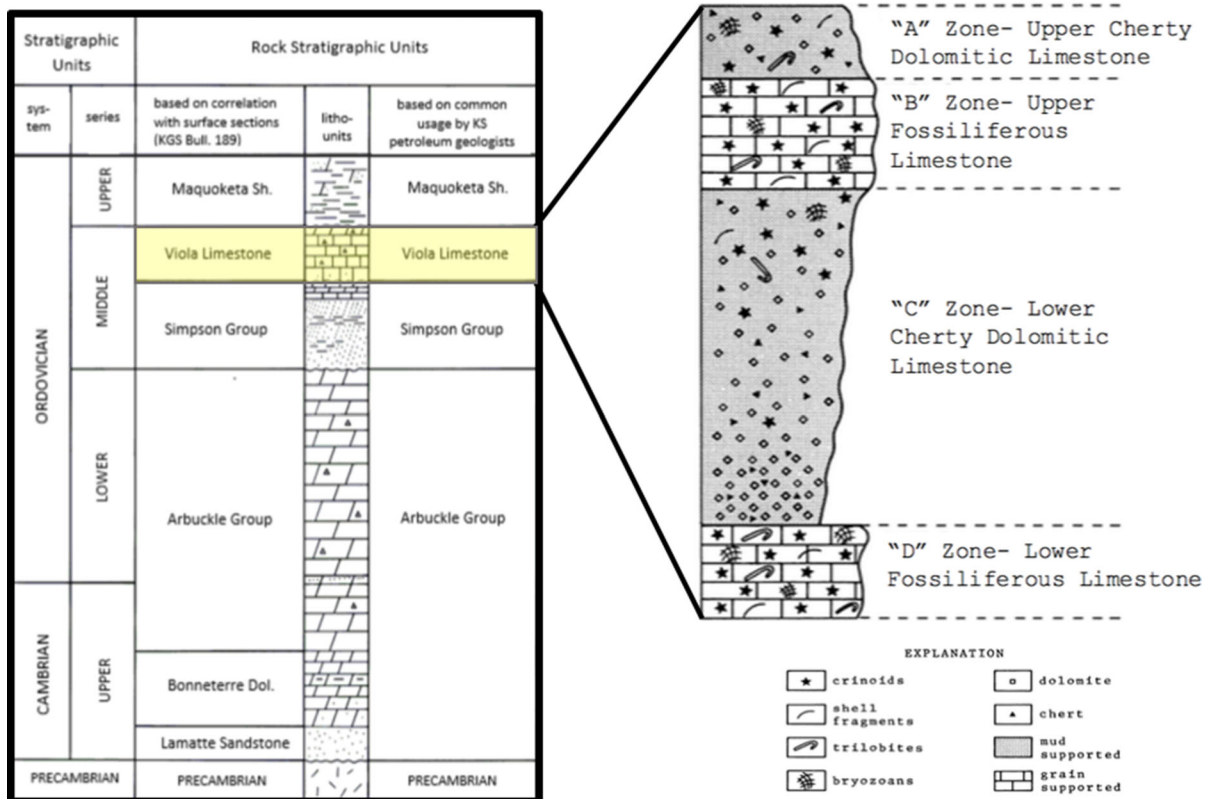
Figure 4
Stratigraphic column showing formations of interest in the study area and the four distinct lithofacies within the Viola. (Modified after Cole 1975)

pay have a correspondingly reduced production, or are dry.

3. Data, Methods, and Results

The approach followed with respect to data selected was to collect and utilize all available data of relevance for the study area (about 19 km^2): 3D seismic reflection, wireline logs, and formation tops and production data. Data collected included a 3D P-wave seismic reflection with trace length of 2 s, sampling of 2 ms, natural bin size of 82.5 ft., and dominant frequency of about 30 Hz, and digital wireline logs, formation tops from drilling reports, and production data for the Morrison NE field. Well and production data are available from the Kansas Geological Survey website. The P-wave, surface, 3D

seismic reflection survey consists of 320 inlines and 380 crosslines with a sampling rate of 2.0 ms, covering about 7.5 mi^2. The seismic survey was processed to a reference datum of 2200 ft. with a replacement velocity of 11,000 ft./s. The projection system used to load the survey was NAD27 Kansas State Planes, Southern Zone, US Foot.

3.1. Well-to-Seismic Tie and Seismic Attributes Versus Porosity Cross Plots

The primary purpose of the one-dimensional synthetic seismic modeling, in this study, is to establish the seismic reflection event (peak in this case) which corresponds to the top of the Viola formation. A secondary purpose is to estimate a representative seismic wavelet, so that we could

investigate tuning effects, which is of interest due to having interpretation value, explained below. Convolutional Synthetic seismic traces, utilizing sonic logs and density logs for impedance and in turn zero-offset reflectivity calculation, have been calculated separately for seven wells based on convolution of extracted seismic wavelets and reflectivity series. These synthetic seismograms were quality checked, and compared and matched to the seismic data (Fig. 5). Two-way seismic time of formation tops was determined, and the corresponding seismic horizons were tracked throughout the area covered by the seismic survey. Tracking horizons throughout the survey enabled the generation of a time structural map for the top of Viola formation.

The Viola formation is seen on the 3D seismic data as peak (impedance increase) with variable amplitude, with lower amplitude associated with
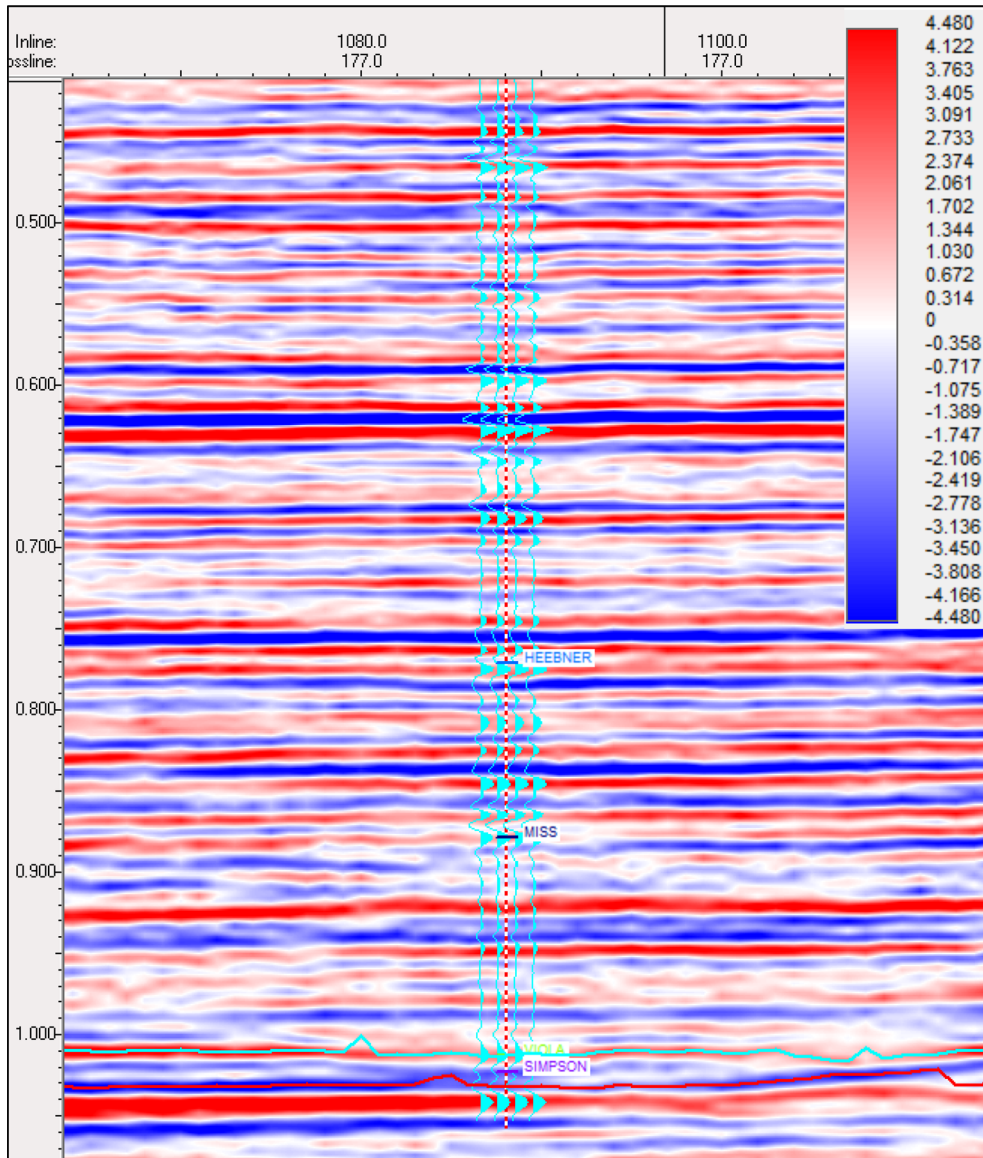

Figure 5
Synthetic-to-seismic tie of Stephens 1. Formation tops and tracked seismic horizons for the Viola and Simpson
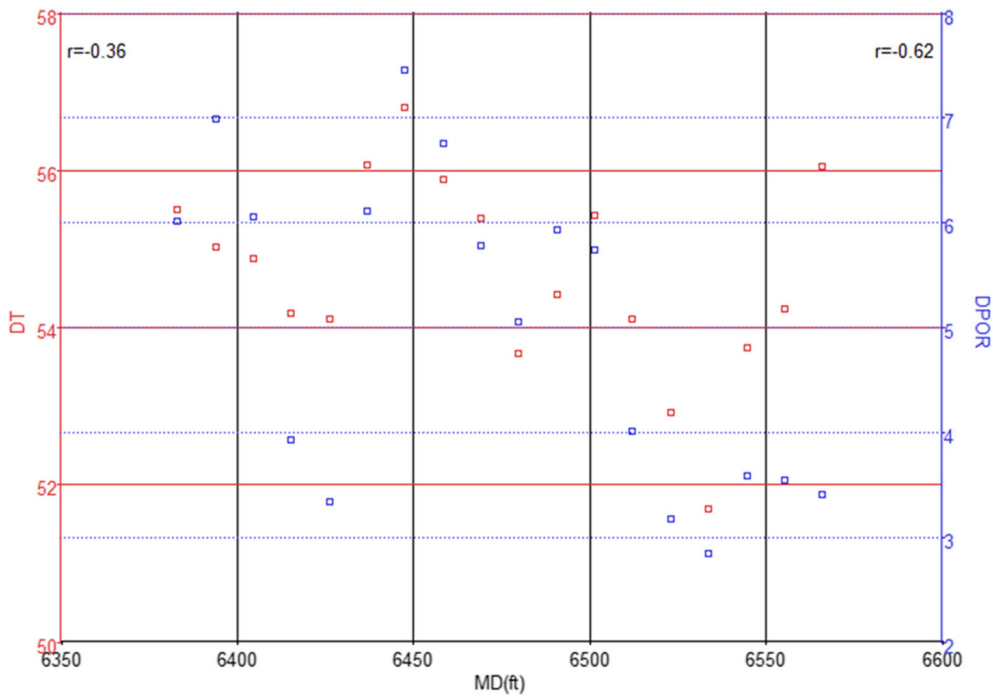
Figure 6
Sonic (DT) and density porosity versus measured depth (MD) for Stephens 1; higher porosity is expected to correlate with lower P-wave velocities (higher DT values)
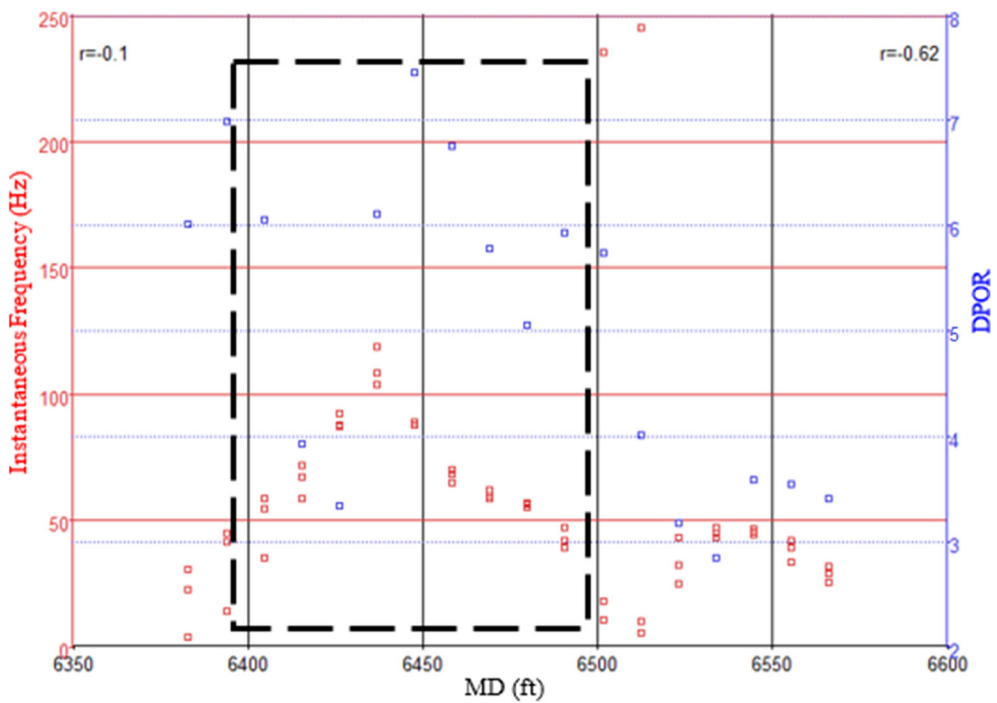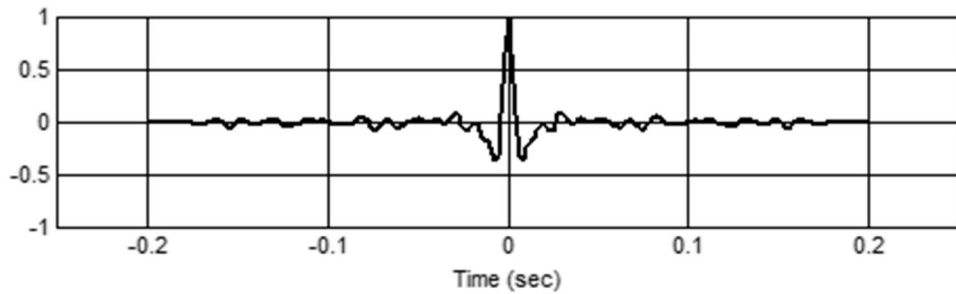

Figure 7
Instantaneous frequency and density porosity versus measured depth for Stephens 1; instantaneous frequency peaking due to the development of thin-layer tuning effects from thin hydrocarbon pay zone—as will be supported further with additional evidence in the following sections
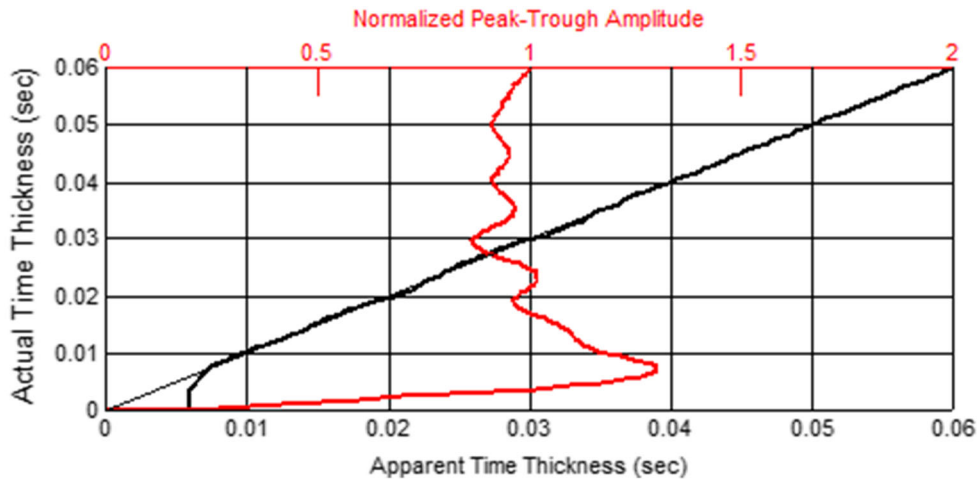
Figure 8
Tuning analysis for dominant seismic wavelet; it is evident that for thicknesses greater than the limit of temporal resolution (7 ms) and smaller than about 50 ms, amplitude decreases with increasing thickness

higher porosity as evident from a cross plot of sonic log (µs/ft.) and density porosity versus measured depth (ft.) within the Viola formation (Fig. 6). As a consequence of the established porosity–sonic trend, amplitude decrease (dimming) with higher porosity is expected. Furthermore, the decrease in velocity in the pay zone, due to both the presence of hydrocarbon and higher porosity, results in higher resolution leading to the development of a seismic doublet event for the Viola top; a situation has been utilized to outline the productive facies based on proxy seismic facies as explained in the following sections.

3.2. Tuning Analysis

For thin layers, the shape and amplitude of the seismic wavelet of a reflection vary in response to interference of reflections from the closely spaced reflecting interfaces. This variation in shape and amplitude is known as the tuning effect (e.g., Kallweit and Wood 1982; Widess 1973). Tuning effects occur when the wavelength is greater than the bed thickness, causing the reflections to resonate and interfere (Hardage 2009). When the bed thickness is one-quarter that of the effective source wavelet or one-half the thickness of the dominant period, there is constructive interference (Chopra and Marfurt 2007). The constructive interference causes a positive amplitude anomaly. In the case of velocity-reducing higher porosity and/or presence of hydrocarbon as evidenced by our data (Figs. 6, 7), increase in time thickness causes the tuning-amplitude contribution to be a decrease for thickness levels from one-fourth of a wavelet to less than a whole wavelet breadth (Fig. 8).
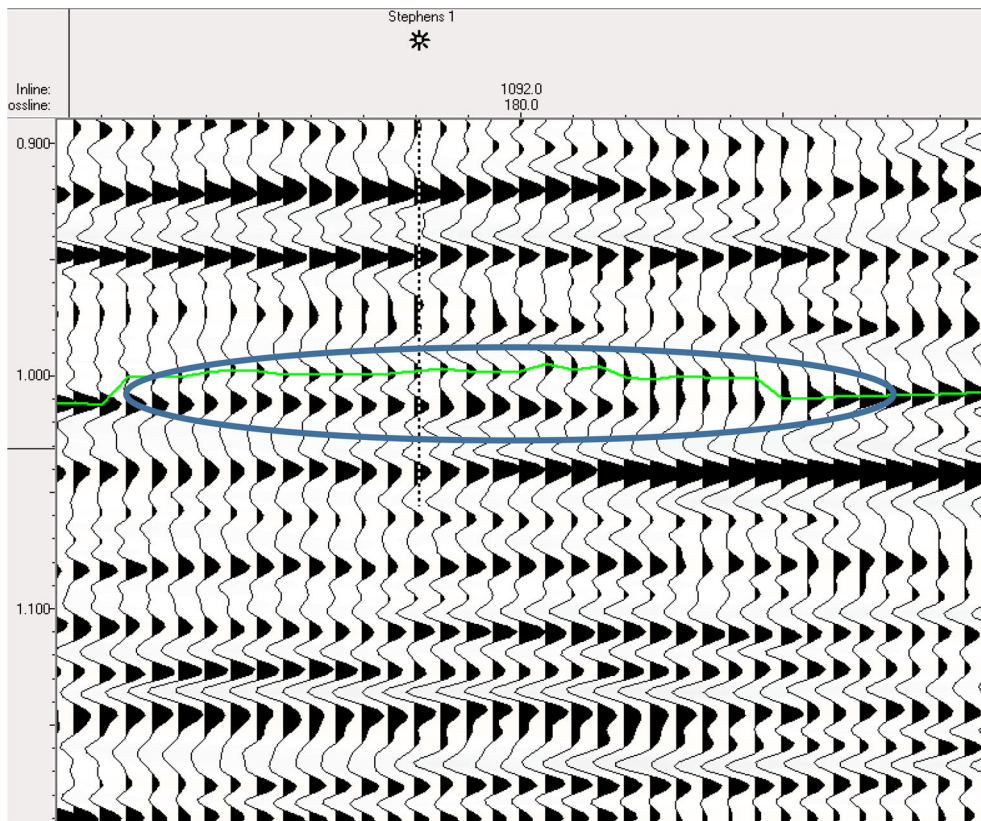
Figure 9
Amplitude wiggle trace cross section with the Viola limestone horizon in green; increased resolution associated with a velocity decrease (hydrocarbon effect) within the Viola leading to separation of the pay zone as a thin layer with the consequence of a seismic doublet event for the Viola top
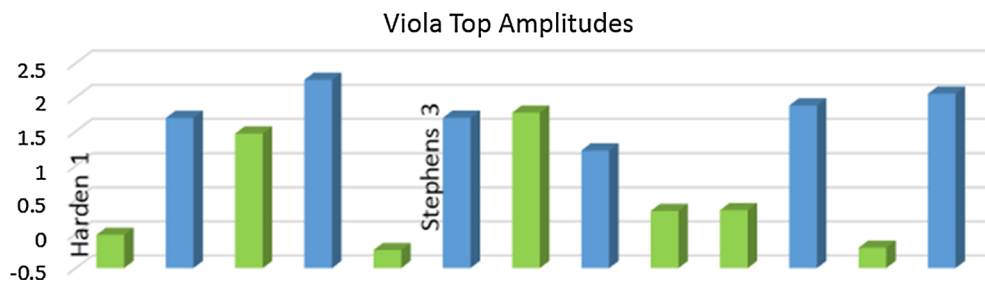

Figure 10
Peak amplitude values for the Viola top horizon at well locations with producing wells in the Viola green and non-producers are blue. Wells are from left to right: Harden 1, Harden 4, Stephens 1, Stephens 10, Stephens 2, Stephens 3, Stephens 4, Stephens 5, Stephens 6, Stephens 7, Stephens 8, Stephens 9, and Stephens "A" 1

In this study, such a situation has been associated with peaking in instantaneous frequency (Fig. 7) due to the splitting into a doublet with tuning interference; such increase occurs in the vicinity of time thickness of one-fourth the dominant wavelet (El-sayed and Slusarczyk 2000, 2001). Unlike hydrocarbon-related instantaneous frequency shadows (Castagna et al. 2003), which is a manifestation
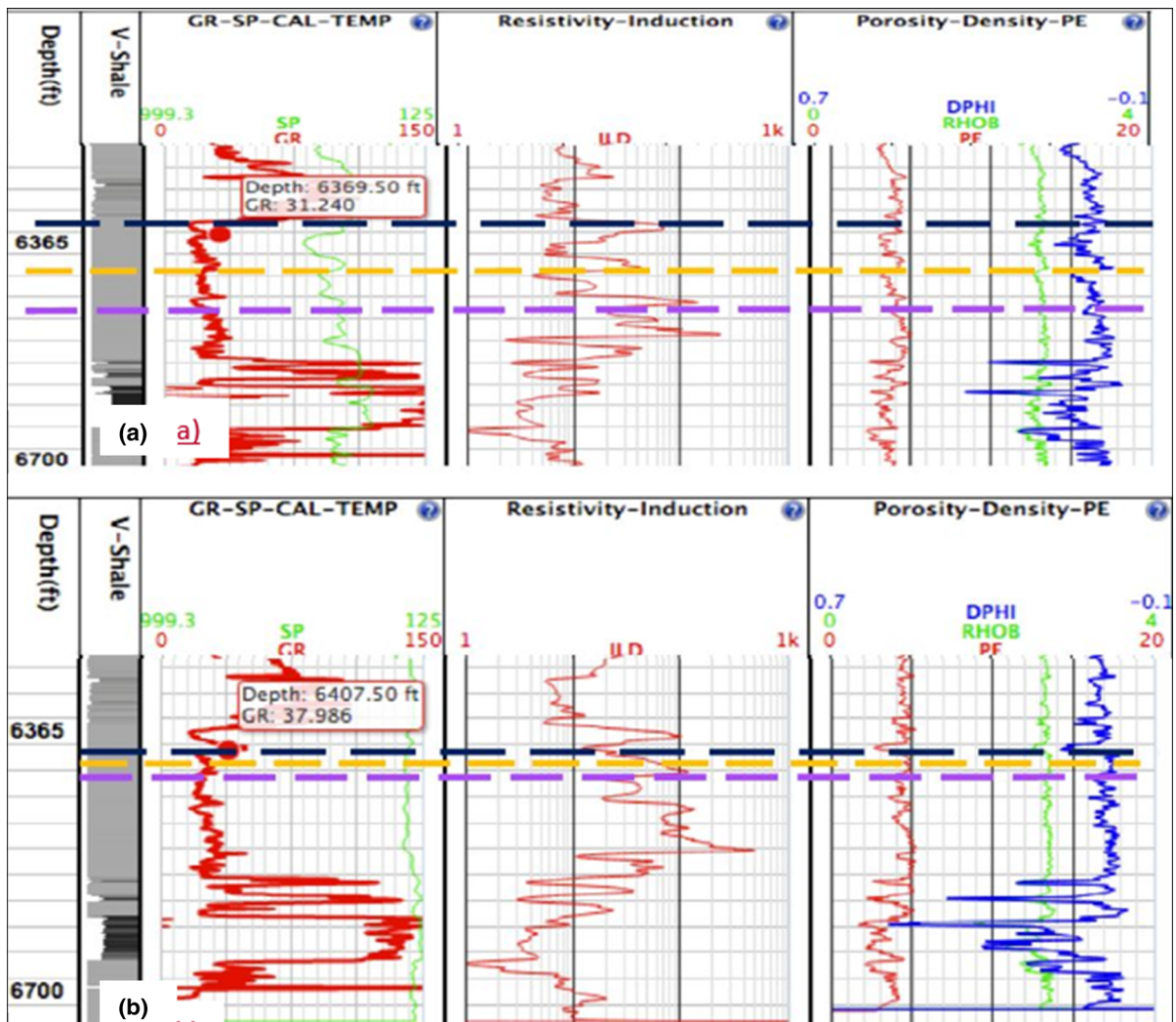
Figure 11

a Well log on Stephens 4 (producer) well. Top of Viola "A" zone marked by black line, Viola "B" zone by yellow line, and Viola "C" zone by purple line. Notice thickness of "A" zone, which is productive interval. **b** Well logs on Stephens 3 (dry hole) well. Line symbols as above. Notice that the Viola "A" zone is almost absent, resulting in non-productive well

of differential attenuation effects, the instantaneous frequency peaking in this study is tuning-related effect resulting from waveform interference.

3.3. 3D Seismic Amplitude and Instantaneous Frequency Facies and Correlation with Productive Lithofacies

Complex trace seismic attributes, including instantaneous frequency, have been known since introduced by Taner et al. (1979). The utilization of the instantaneous frequency in reservoir characterization, for thin beds in particular, has been shown by Zeng (2010). The response of complex seismic trace attributes of a wedge model has been reported by Elsayed and Slusarczyk (2000). Instantaneous frequency increases as interference of bottom and top reflections and continues as thickness decrease beyond one-fourth of a wavelength.

The choice of seismic attributes for analysis, in this study, has been guided by both the productive facies' thickness (thin-layer effects)—increasing
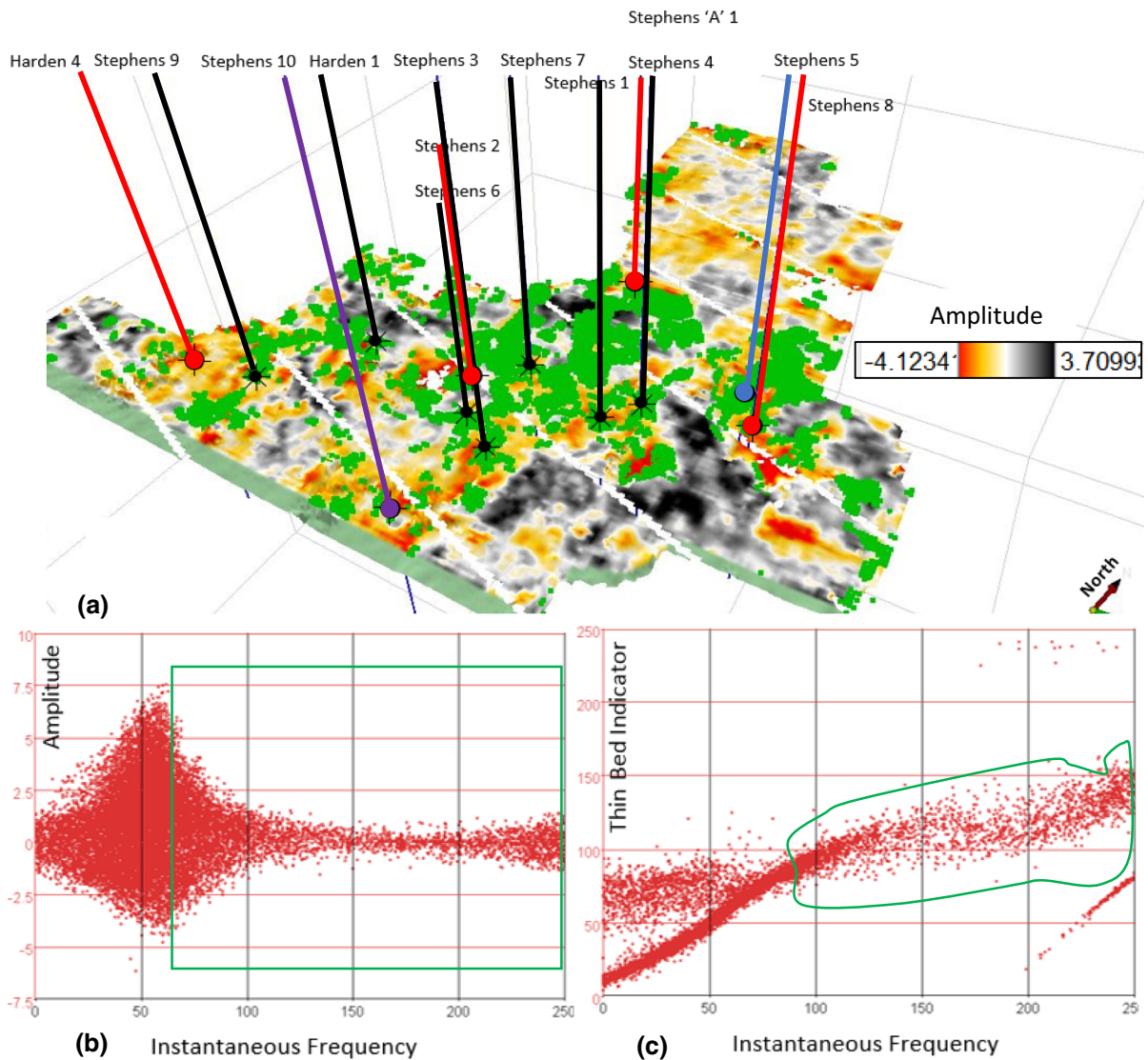
Figure 12

a Horizon amplitude map of the Viola, **b** instantaneous frequency–amplitude, and **c** instantaneous frequency-thin bed indicator; wells producing from the Viola are displayed in black, dry holes drilled in the Viola are displayed in red and the saline water disposal well is in blue, and the purple well produces from the Morrow formation and was originally a dry hole targeting the Viola. A good correlation can easily be seen between the seismic facies, posted in green color on the amplitude map (marked with light green box on both cross plots) and the producing wells

apparent time thickness with increasing porosity and higher hydrocarbon saturation—and the associated higher resolution with decreasing seismic _P-wave velocity. The thin-layer effects and the lowering velocity, for the target zone under investigation, resulted in a combined effect of decreasing peak amplitude and the development of a doublet event (Fig. 9) for the Viola top with the pay zone separating as a thin layer. Amplitude decrease with the presence

of hydrocarbon reservoir facies is evident from the bar diagram, as shown in Fig. 10.

Comparison of the pay zone ("A" zone) thickness of the Viola at Stephens 4 (a producer) and Stephens 3 (dry hole) (Fig. 11a, b) provides evidence that the thickness of the reservoir facies ("A" zone) is an essential controlling factor in the study area. An increased thickness of the reservoir facies correlates with lower seismic amplitudes (Fig. 10); the "A"
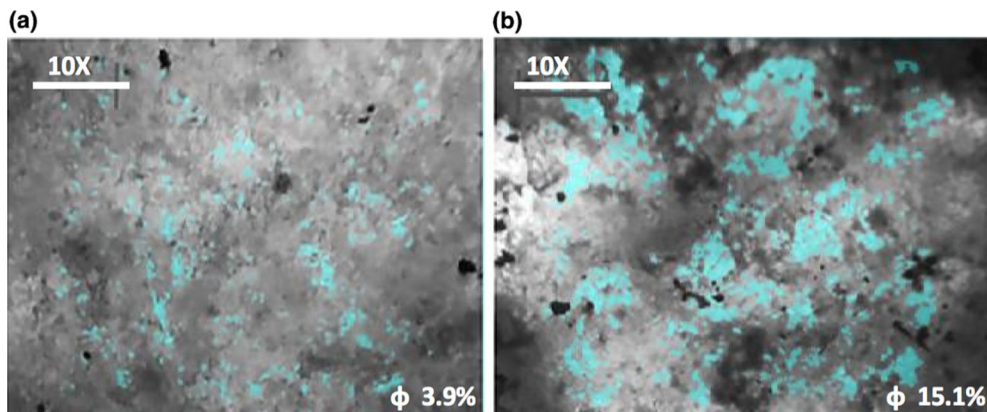
Figure 13
Grey scale petrographic images with porosity (enhanced epoxy) at 10X of Stephens 3 well (dry hole) on the left (**a**) and Harden 1 well (producer) on the right (**b**). Significant contrast in porosity are clearly exhibited between the Stephens 3 well and Harden 1 wells, as Stephens 3 portrays low porosity (3.9%), while the Harden 1 well exhibits good vuggy porosity (15.1%). These examples represent the two separate facies observed in the field

zone is about 25-feet thick at Harden 1. Even thicker "A" zone, as shown in Stephens 4 (Figs. 10, 11a), where the pay zone is about 68-feet thick, the expected tuning contribution causes amplitude to increase compared to at wells with thinner pay zone. In general, a decreasing amplitude and a surge in instantaneous frequency values are expected as a result of the combined effect of lower velocity and the thin-layer interference. This effect can be used as a proxy of hydrocarbon reservoir facies. An example of the increase of instantaneous frequency in response to thin reservoir layers has been correlated with numbers of zero-crossings for a shale dominated sequence (e.g., Brown 2011). In this case study (the Stephens Ranch lease), the pay zone is thin, so when it is present, the instantaneous frequency surges (Fig. 12a, b). The higher instantaneous frequency is correlating with higher thin bed indicator (Fig. 12c). In the following sub-section, a petrographic comparison of the seismic (reservoir) facies and the non-productive facies is presented.

3.4. Petrographic Aspects of the Reservoir and Non-Reservoir Lithofacies of the Viola Formation

The correlation between the well logs and the seismic facies recognizing the presence or absence of the productive Viola "A" facies was examined petrographically. Cores were not available in the study area; hence, drill-cuttings were obtained from available wells, impregnated with blue epoxy, and made into thin sections. A petrographic microscope was used to determine the general mineralogy as well as the structural fabric. The non-productive lithofacies (e.g., Fig. 13a) lacked connected porosity, whereas the reservoir facies manifested good vuggy and fracture porosity (e.g., Fig. 13b). These two lithofacies represent the different seismic facies (green and non-green), as represented in Fig. 12. Description of the thin sections from these wells is presented in Table 1.

Thin sections were also examined under SEM. Examples are shown in Fig. 14, where the reservoir facies show good fracture and vuggy porosity, while the non-productive facies (Fig. 15) show poor porosity.

4. Discussion

Given that the Viola top corresponds to a peak in a normal "positive" polarity data (Fig. 5) and the sonic well-log values increase with increasing porosity (Fig. 6), the lower amplitude for the

Table 1

Description of lithofacies from non-productive and productive wells

Well	Cuttings description	Thin section description	Overall porosity (%)
Stephens 3	Gray tabular shale/limestone dominant; planar fractures in shale prominent; more red clay present; more {and huge} milky/bone white chert with very jagged edges present; not as much sucrosic dolomite present; still have a good bit of microcrystalline limestone (with minor staining); pyritic; no shows noted	Packstone dominant; prominent gray shale; minor dolomite present with subhedral–euhedral rhombs; chert much more prevalent; prominent pyrite present; very low porosity overall	3.9
Harden 1	Limestone gray lt gray dominant with planar fracture; more microcrystalline creamy white limestone; some pyritic. Less sucrosic brown dolostone; more argillaceous green/gray limestone; minor red clay; minor glauconite; chert present; anhydrite more prevalent	Grainstone dominant; allochems include forams and bryozoan; pyritic; dolomite more anhedral rhombic with intercrystalline and vuggy porosity; minor glauconite; some packstone present with good interparticle and fracture porosity	15.1
Stephens 4	Dense microcrystalline limestone cream gray dominant; fair sucrosic dolomite present; minor saturated stain; off white cream sharp, jagged chert present; fair porosity visible; no shows noted	Fossiliferous limestone packstone/grainstone dominant; some iron oxide staining on dolomite; minor chert; not as nearly as much shale present; porosity visible along fractures; notable vuggy porosity also present; porosity seems to be along edges of grains; more fracture fabric supported porosity present	20.5

reservoir facies is well justified for this case study. This observation is further corroborated when comparing amplitude at producers with that at dry holes (Fig. 10). Figure 7 provides evidence on that instantaneous frequency clearly surges in the pay zone. The spatial correlation of higher instantaneous frequency (Fig. 12) highlights the point that what has been evidenced by cross-plotting density porosity versus instantaneous frequency for Stephens 1 is applicable to the entire area of study.

This case study presents an example of utilizing the sensitivity of instantaneous frequency to the thin pay zone as a proxy to hydrocarbon presence. This utilization has been greatly assisted by the increased resolution due to velocity decrease as was evidenced by a doublet response for the Viola top. Time structural maps (Fig. 16) on the top the Viola; one time tracking the upper half of the doublet (lower map in Fig. 16) and another time tracking the lower peak of the doublet, indicate strong correlation of the doublet with the productive facies. This pay zone is successfully outlined based on a low amplitude and higher instantaneous frequency seismic facies. These seismic facies are clearly an outcome of the combined effect of pay zone thickness (thin-layer effects)

and increase of temporal resolution as a result of lower velocities caused by hydrocarbon and higher porosity effects.

5. Conclusions

Previous work by Richardson (2013) explains varying thickness in the Viola as it relates to preserving the productive porosity in a paleotopographic trap. In our approach of outlining areas with productive facies (Viola "A" zone), we adopted low amplitude, high instantaneous frequency seismic facies with meaningful correlation with the reservoir facies as evidenced by drilling results, and SEM scans, and petrographic images of reservoir facies. The calibrated seismic facies can also be used in outlining thin sands in intervals of shale or carbonates as long as the sand time thickness less than one wavelet breadth.

The wells associated with higher production rates exhibit both diagnostic dolostone and packstone/grainstone facies with prominent vuggy porosity along with seismic response of lower amplitudes and higher instantaneous frequency than
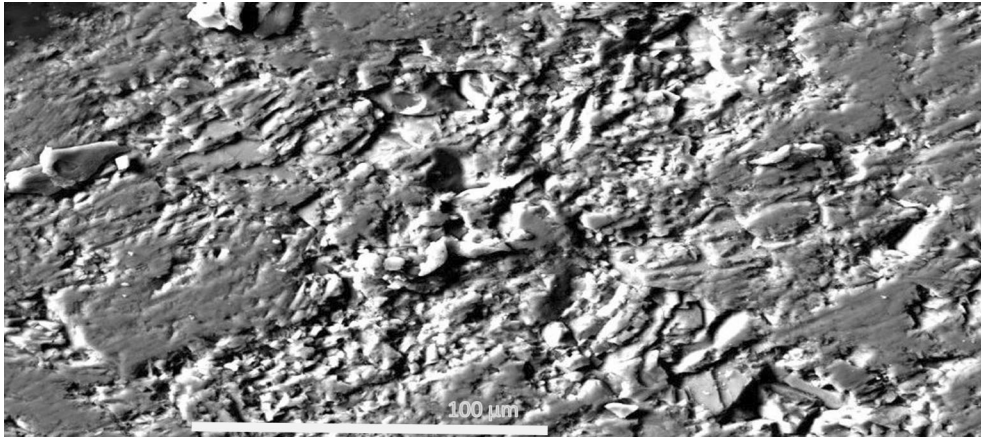
Figure 14
SEM image of Stephens 4 well (producer). Significant fracture and vuggy porosity are clearly exhibited. This example represents the Viola "A" facies
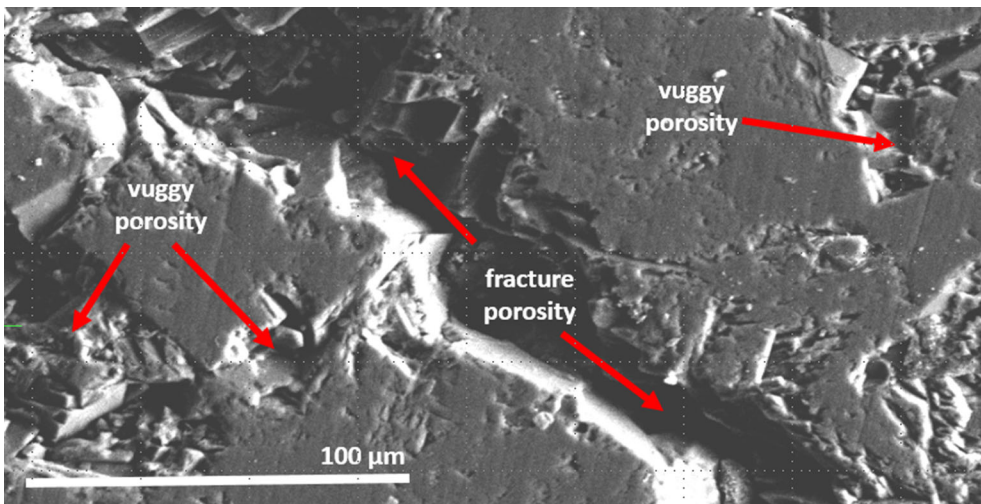

Figure 15
SEM image of Stephens 3 well (dry hole). Note relative lack of porosity. This example represents the Viola "C" facies

the non-reservoir facies. Integration of other independent data such as petrographic images, SEM scans, and well-log facies has validated the pay-zone seismic facies for use in deciding on future well placement.
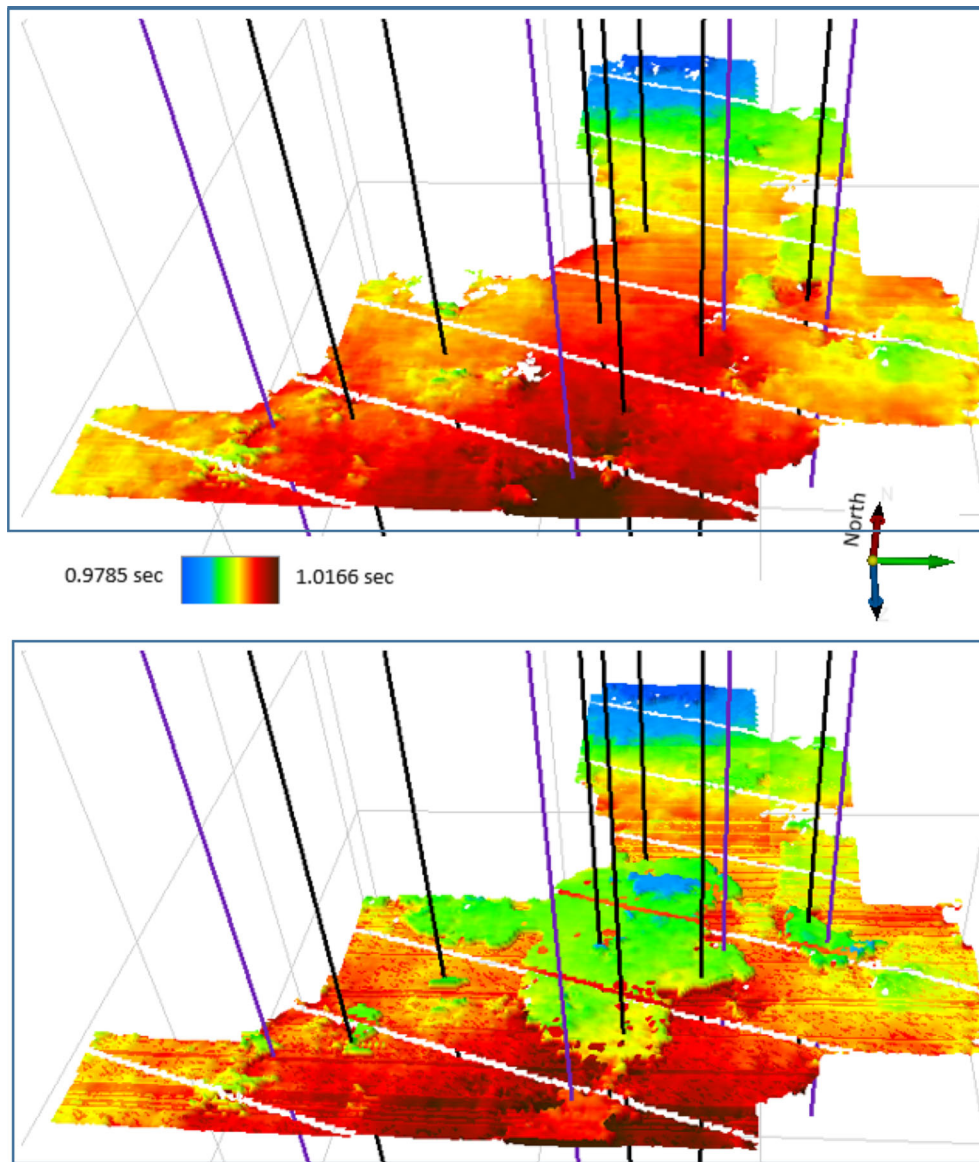
Figure 16

Structural time maps for Viola top with tracking the lower peak of of the doublet split when present (upper time horizon) and with tracking the upper peak of the doublet (lower map); production wells (black) are associated with the presence of the doublet as evident from correlating the difference with the locations of the unsuccessful (purple lines) and successful (black lines) wells

REFERENCES

Adkinson, W. L. (1972). Stratigraphy and structure of middle and upper ordovician rocks in the sedgwick basin and adjacent areas, South-Central Kansas. Geological Survey Professional Paper 702.

Bornemann, E., Doveton, J. H., & St. Clair, P. N. (1982). Lithofacies analysis of the Viola Limestone in South-central Kansas: Kansas Geol. Survey. *Petrophysical Series, 3,* 50.

Brown, A. R. (2011). Interpretation of three-dimensional seismic data. AAPG Memoir 42, SEG Investigations in Geophysics (pp. 286–287).

Bunt, R. J. W. (2015). The use of seismic attributes for fan and reservoir definition in the Sea Lion Field. *North Falkland Basin. Petroleum Geoscience, 21*(2–3), 137–149.

Castagna, J. P., Siegfried, R. W., & Sun, S. (2003). Instantaneous spectral analysis: detection of low frequency shadows associated with hydrocarbons. *The Leading Edge, 22,* 120–127.

Chen, Q., & Sidney, S. (1997). Seismic attribute technology for reservoir forecasting and monitoring. *The Leading Edge, 16*(5), 445–448.

Chopra, S., & Marfurt, K. J. (2007). Seismic attributes for prospect identification and reservoir characterization. SEG Geophysical Development Series No. 11. Tulsa: Society of Exploration Geophysicists.

Chopra, S., & Marfurt, K. J. (2008). Emerging and future trends in seismic attributes. *The Leading Edge, 27*(3), 298–318.

Cole, V.B. (1975). Subsurface Ordovician-Cambrian rocks in Kansas with maps showing the thickness of potentially oil-bearing formations. Subsurface Geology Series 2 (p. 18). Lawrence, USA: Kansas Geological Survey.

Coléou, T., Poupon, M., & Azbel, K. (2003). Unsupervised seismic facies classification: a review and comparison of techniques and implementation. *The Leading Edge, 22*(10), 942–953.

Elsayed, R. E. (2001). Seismic modeling and multi attribute analysis—Guiding applications of 3D seismic attributes to reservoir characterization. University of Science and Technology, PhD-Thesis, Cracow, Poland, pp. 20–26.

Elsayed, R. A., & Ślusarczyk, R. (2000). Analysis of seismic attributes responses to a thinning layer. *Romanian Geophysics,* 7(Suppl. 1).

Goebel, E. D. (1968). Mississippian rocks of western Kansas. *American Association of Petroleum Geologists Bulletin 52,* 1732–1778.

Hardage, B. A. (2009). Frequencies are fault finding factors: looking low aids data interpretation. *AAPG Explorer, 30*(9), 34.

http://www.kgs.ku.edu/PRS/County/abc/clark.html. Accessed Sept 2016.

IHS Global Inc. (2012). Rock solid attributes, Version 8.7.

Kallweit, R. S., & Wood, L. C. (1982). The limits of resolution of zero-phase wavelets. *Geophysics, 47,* 1035–1046.

Raef, A. E., Mattern, F., Philip, C., & Totten, M. W. (2015). 3D seismic attributes and well-log facies analysis for prospect identification and evaluation: interpreted palaeoshoreline implications, Weirman Field, Kansas, USA. *Journal of Petroleum Science and Engineering, 133,* 40–51.

Raef, A. E., Meek, T. N., & Totten, M. W. (2016). Applications of 3D seismic attribute analysis in hydrocarbon prospect identification and evaluation: verification and validation based on fluvial palaeochannel cross-sectional geometry and sinuosity, Ness County, Kansas, USA. *Marine and Petroleum Geology, 73,* 21–35.

Richardson, L. J. (2013). The Herd Viola trend, Comanche County, Kansas. AAPG Search and Discovery Article #20220.

Sheriff, R. E., & Geldart, L. P. (1995). *Exploration seismology.* Cambridge: Cambridge University Press.

St. Clair, P. N. (1981). Depositional history and diagenesis of the Viola Limestone in south-central Kansas: Unpub. M.S. thesis, University of Kansas, p. 66.

Taner, M. T. (2001). Seismic attributes, rock solid images, Houston, TX, USA. CSEG Recorder, September, 2001, pp. 48–56.

Taner, M. T., Koehler, F., & Sheriff, R. E. (1979). Complex seismic trace analysis. *Geophysics, 44*(6), 1041–1063.

Wang, Z., Gao, J., Lei, X., Cui, X., & Wang, D. (2016). Application of 3D seismic attributes to optimize the placement of horizontal wells within a tight gas sand reservoir, Ordos Basin, China. *Geophysics, 81*(3), B77–B86.

Widess, M. B. (1973). How thin is a thin bed? *Geophysics, 38,* 1176–1180.

Zeng, H. (2010). Geologic significance of anomalous instantaneous frequency. *Geophysics, 75*(3), P23–P30.